ELSEVIER

Chemical Engineering Science ▮▮▮ (▮▮▮▮) ▮▮▮–▮▮▮

Chemical Engineering Science

www.elsevier.com/locate/ces

Multiphase mass transport with partitioning and inter-phase transport in porous media

F.A. Coutelieris[a,b,*], M.E. Kainourgiakis[b], A.K. Stubos[b], E.S. Kikkinides[a,c], Y.C. Yortsos[d]

[a]*Department of Engineering and Management of Energy Resources, University of Western Macedonia, Bakola & Sialvera, 50100 Kozani, Greece*
[b]*National Center for Scientific Research "Demokritos", 15310 Aghia Paraskevi Attikis, Greece*
[c]*Center for Research and Technology Hellas, Chemical Process Engineering Research Institute, 57001 Thermi, Thessaloniki, Greece*
[d]*Department of Chemical Engineering, University of Southern California, Los Angeles, CA 90089-1211, USA*

Received 13 October 2005; received in revised form 28 February 2006; accepted 28 February 2006

Abstract

We consider deriving the effective mass-transfer coefficient between two fluid phases in a porous medium, one of which is flowing and the other is immobile. A passive tracer is advected by the flowing phase, becomes partitioned at the fluid–fluid interface and diffuses in the immobile phase. We use traditional volume-averaging methods to obtain a unit-cell boundary-value problem for the calculation of the effective mass-transfer coefficient. The problem is controlled by the Peclet number of the flowing phase, by a second dimensionless parameter that captures diffusion and partition in the two phases and by the geometrical properties of the porous medium.

We derive asymptotic results for the scaling of the mass-transfer coefficient under various limiting conditions. Then, we use numerical methods that solve for the flow velocity field under Stokes flow conditions, and for the transport problem. The numerical results verify the asymptotic scaling expressions and provide estimates of the coefficient for a number of special cases. In particular, we find that when the immobile phase is wetting the solid (in the form of films), the mass transfer coefficient is larger than in the non-wetting case (where the phase is distributed in the form of blobs). Shape factors for practical applications are also obtained.

Keywords: Advection; Dispersion; Mass transfer; Interphase equilibria; Multiphase flow; Porous media

1. Introduction

There are numerous physicochemical processes, where an aqueous phase coexists and/or interacts with a non-aqueous liquid phase in a porous medium. Many are of significant importance in terms of industrial and technological applications. For typical examples, we cite tracer transport in petroleum reservoirs, the contamination of soils or aquifers by chemical products, the long-term interaction between liquefied or chilled foods with packaging materials, and many others. The description of such processes often relies on mathematical models as experimentation can be expensive or difficult.

In the presence of porous media, the need for a realistic description of the structure of a porous medium significantly increases the mathematical complexity of a model. However, elements of the microstructure must be captured when moving from the pore level to the macroscopic level, where often the process performance must be studied. A number of techniques for the upscaling from the pore-scale to the macroscopic scale in porous media have been developed. Of specific interest to this paper is volume-averaging (Plumb and Whitaker, 1990; Carbonell and Whitaker, 1984; Zanotti and Carbonell, 1984a,b), which is very useful when pore scales and macroscopic scales are separated. Starting from the relevant differential equations at the pore level and using the spatial averaging theorem, one is led after several mathematical manipulations, based on scale separation (Whitaker, 1967, 1977), to unit-cell problems for the estimation of macroscopic quantities (Quintard and Whitaker, 1993a,b). Spatial averaging techniques allow for the integral effect of the influence of

* Corresponding author. Department of Engineering and Management of Energy Resources, University of Western Macedonia, Bakola & Sialvera, 50100 Kozani, Greece. Tel.: +30 2461056751; fax: +30 2106525004.
E-mail addresses: fcoutelieris@unwm.gr, frank@ipta.demokritos.gr (F.A. Coutelieris).

0009-2509/$ - see front matter © 2006 Published by Elsevier Ltd.
doi:10.1016/j.ces.2006.02.037

pore geometry on transport to be captured in the mathematical formulation.

The present paper deals with the specific case of tracer transport in a multiphase environment. Typically, the macroscopic models involve an exchange term to describe the rate of mass transfer between the two phases. The solution of the macroscopic equations requires the knowledge of several macroscopic constants (e.g., the mass transport coefficient and the dispersion tensor). In general, one uses empirical correlations of the latter as a function of the Sherwood or the Peclet number, obtained from experimental measurements of specific systems (e.g. see Quintard and Whitaker, 1994). From a theoretical perspective, estimating these quantities is also possible using techniques, such as volume averaging (Whitaker, 1967, 1977). The majority of previous theoretical works derive such models based on the assumption of mass exchange equilibrium between the aqueous and the non-aqueous liquid phases, as discussed at length in previous works (Hunt et al., 1988; Fried et al., 1979; Geller and Hunt, 1993; Lam et al., 1983). This assumption of infinitely fast diffusion in the non-aqueous phase, simplifies the mathematical modeling and the consequent simulation effort (Quintard and Whitaker, 1994; De Smedt and Wierenga, 1979; Gvirtzam et al., 1988). In the present work, we probe the validity of this assumption. When the assumption is relaxed, the resulting unit-cell problem includes mass transport between the two phases (the "aqueous" and the "non-aqueous" liquids), thus accounting for inter-phase diffusion and partitioning. Its solution provides needed expressions for the macroscopic mass-transfer coefficient. We use various model pore geometries to obtain representative results. An ab initio calculation is also presented, in which the Stokes equations are solved in typical pore geometries and compared with the volume-averaging results.

2. Background

Consider a multi-phase domain consisting of a flowing aqueous phase (β-phase), an immobile non-aqueous liquid phase (γ-phase) and a solid phase (σ-phase), as schematically depicted in Fig. 1. The assumption of a motionless γ-phase is a good approximation for several applications such as water or gas tracer transport in hydrocarbon reservoirs where the oil phase rests practically immobile (e.g. residual saturation), slow dissolution of NAPL's in underground porous formations, and the packing of porous pellets with the presence of a wetting fluid. To relax this assumption, one should recourse to techniques like Lattice-Boltzmann which are capable of solving the flow problem while simultaneously determining the dynamic distribution of fluid phases in the considered porous domain (requiring however significant computational resources (Bekri and Adler, 2002). A partitioning tracer is advected by the flowing β-phase and partitioned in the immobile phase into which it is diffusing. It is also assumed that the solid phase is physico-chemically neutral, i.e., the tracer is neither adsorbed nor reacts with the σ-phase. The governing processes are diffusion and advection in the β-phase, and diffusion in the γ-phase. The mass exchange at the $\beta\gamma$ interface is characterized by the diffusion and partitioning properties of the tracer. The macroscopic

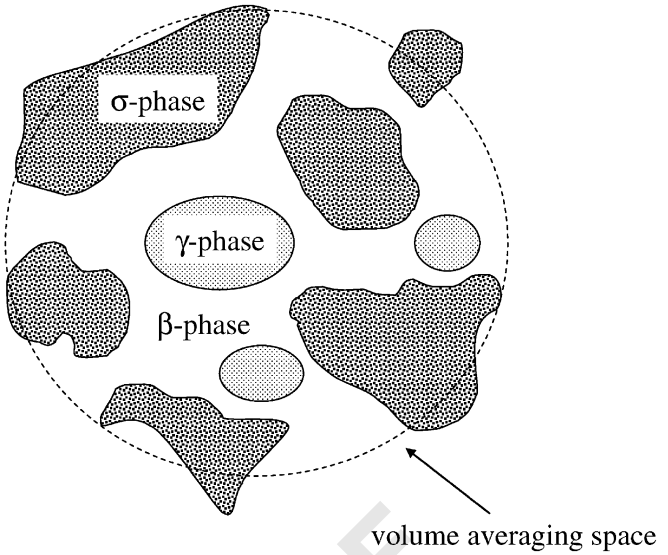

Fig. 1. Schematic of a typical representative volume.

modeling of the processes is typically described by the following advection–dispersion–reaction equations:

$$\varepsilon_\beta \frac{\partial \langle C_\beta \rangle}{\partial t} + \langle \mathbf{v} \rangle \cdot \nabla \langle C_\beta \rangle = \varepsilon_\beta D_\beta^* \nabla^2 \langle C_\beta \rangle - \alpha \left(\langle C_\beta \rangle - \frac{1}{K} \langle C_\gamma \rangle \right), \tag{1}$$

$$\varepsilon_\gamma \frac{\partial \langle C_\gamma \rangle}{\partial t} = \varepsilon_\gamma D_\gamma^* \nabla^2 \langle C_\gamma \rangle + \alpha \left(\langle C_\beta \rangle - \frac{1}{K} \langle C_\gamma \rangle \right), \tag{2}$$

where ε_β, ε_γ denote the volume fraction of the β- and γ-phase, respectively, $\mathbf{v}$ is the velocity vector in the β-phase, D_β^*, D_γ^* are the macroscopic dispersion coefficients in the β- and γ-phase, respectively, and K is the partitioning coefficient. Brackets denote averages, such that for any function y_i associated with the i-phase (either β or γ), the superficial volume average is defined as

$$\langle y_i \rangle = \frac{1}{V} \int_{V_i} y_i \, \mathrm{d}V \tag{3}$$

and the interstitial volume average as

$$\langle y_i \rangle^i = \frac{1}{V_i} \int_{V_i} y_i \, \mathrm{d}V. \tag{4}$$

By V we denote the total volume of the porous material, with V_β and V_γ being the volumes of aqueous and non-aqueous phases, respectively.

The solution of the above macroscopic equations requires the knowledge of several parameters (e.g., of the mass-transfer coefficient and the dispersion tensor). As we noted, volume averaging is a useful approach for providing these expressions when scale separation exists. The main theoretical work in this field is of Quintard and Whitaker (1994), which provided methods for the calculation of the mass-transfer coefficient and the dispersion tensor under the assumption of infinitely fast diffusion in the γ-phase. As we noted above, this corresponds to an

almost-constant concentration profile in the γ-phase and permits the decoupling of the mass transport problems in the two phases. Mass exchange between the two phases has been also modelled by considering either a controlling diffusive process, macroscopically described by first-order kinetics, or by an advection process (Ahmadi et al., 1998; Gwo et al., 1998; Vogel et al., 2000; Dagan and Lessoff, 2001; Lessoff and Dagan, 2001; Bekri et al., 1997). Here, we will propose a more rigorous extension by considering non-equilibrium partitioning of the tracer in the two phases and mass transfer in both phases. In the numerical illustrations to be shown, we will consider 3-D model pore geometries, where the immobile γ-phase may be distributed either in the form of wetting films or in the form of non-wetting aggregates (blobs). We seek to obtain estimates of the mass transport coefficient and to investigate the effect of different structural and physicochemical parameters under non-equilibrium partitioning. Otherwise, the volume averaging approach we apply is conventional and consists of the following algorithm:

- Solve the flow problem at the pore level and calculate interstitial and superficial velocity fields.
- Formulate the mass transport problem at the pore level.
- Decompose the local velocities and concentrations in terms of interstitial averages and fluctuations.
- Describe the concentration fluctuations in terms of linear combinations of interstitial averaged concentrations and their gradients.
- Solve closure problems.
- Integrate the resulting quantities to calculate macroscopic coefficients.

3. Formulation of the problem

The pore-level transport of the tracer in the β-phase is described by the diffusion–advection equation

$$\frac{\partial C_\beta}{\partial t} + \nabla \cdot (\mathbf{v} C_\beta) = D_\beta \nabla^2 C_\beta, \tag{5}$$

where C_β is concentration, t is time, $\mathbf{v}$ is the fluid velocity and D_β is the diffusivity in the β-phase. Since the γ-phase is assumed immobile, the diffusion equation describes the transport of tracer in that phase

$$\frac{\partial C_\gamma}{\partial t} = D_\gamma \nabla^2 C_\gamma, \tag{6}$$

where C_γ and D_γ are concentration and diffusivity in the γ-phase, respectively. Zero-flux boundary conditions apply on the solid–liquid interfaces

$$\mathbf{n}_{\beta\sigma} \cdot \nabla C_\beta = 0 \quad \text{at } A_{\beta\sigma}, \tag{7}$$

$$\mathbf{n}_{\gamma\sigma} \cdot \nabla C_\gamma = 0 \quad \text{at } A_{\gamma\sigma}, \tag{8}$$

as the transported species does not absorb or react at the solid. At the interface $A_{\beta\gamma}$ between trapped and flowing phases, the following conditions apply

$$C_\gamma = K C_\beta, \tag{9}$$

$$D_\beta \mathbf{n}_{\beta\gamma} \cdot \nabla C_\beta = D_\gamma \mathbf{n}_{\beta\gamma} \cdot \nabla C_\gamma, \tag{10}$$

where K is the partitioning coefficient. Eq. (9) describes partition equilibrium, while (10) expresses flux continuity at the interface. This description of mass exchange is more general than in previous works (Quintard and Whitaker, 1994) and does not make use of the assumption of fast diffusion in the γ-phase as used in Quintard and Whitaker (1994), De Smedt and Wierenga (1979), Gvirtzam et al. (1988).

Following the volume-averaging procedure (Quintard and Whitaker, 1994), local concentrations and velocities are next decomposed into interstitial averages and fluctuations

$$C_\beta = \langle C_\beta \rangle^\beta + C'_\beta, \tag{11a}$$

$$C_\gamma = \langle C_\gamma \rangle^\gamma + C'_\gamma, \tag{11b}$$

$$\mathbf{v}_\beta = \langle \mathbf{v}_\beta \rangle^\beta + \mathbf{v}'_\beta, \tag{11c}$$

which subsequently are substituted in the governing differential equations. Invoking separation of scales to discard small terms, linearizing and proceeding as in Quintard and Whitaker (1994) we obtain, assuming an isotropic medium of uniform porosity and constant volume fractions, the following representation

$$C'_\beta = \mathbf{b}_\beta \cdot \nabla \langle C_\beta \rangle^\beta + s_\beta \left(\frac{1}{K} \langle C_\gamma \rangle^\gamma - \langle C_\beta \rangle^\beta \right), \tag{12a}$$

$$C'_\gamma = \mathbf{b}_\gamma \cdot \nabla \langle C_\gamma \rangle^\gamma + s_\gamma \left(\frac{1}{K} \langle C_\gamma \rangle^\gamma - \langle C_\beta \rangle^\beta \right), \tag{12b}$$

where $\mathbf{b}_\beta$, $\mathbf{b}_\gamma$, s_β and s_γ are closure variables satisfying specific boundary value problems. Before proceeding we should note that in general separation of scales may not apply in all non-equilibrium problems. It is guaranteed, but in the non-interesting problem when the macroscopic concentration is equal to its equilibrium value (Kechagia et al., 2002). In the general case the problem is non-local and decomposition (12a) and (12b) do not apply, strictly speaking. Aware of this limitation, we will nonetheless continue with the traditional approach postulated in Quintard and Whitaker (1994) in order to demonstrate the relative effect of non-equilibrium exchange between the two phases.

4. The closure problems

Our main interest is in the mass-exchange coefficient, hence we will avoid discussing the closure problems for $\mathbf{b}_\beta$ and $\mathbf{b}_\gamma$ (for details on the latter, see Quintard and Whitaker (1994)), and we will restrict our attention only to s_β and s_γ. It can be readily shown that variable s_β of the β-phase satisfies the boundary value problem

$$\mathbf{v}_\beta \cdot \nabla s_\beta = D_\beta \nabla^2 s_\beta - \varepsilon_\beta^{-1} \alpha, \tag{13}$$

with boundary conditions

$$s_\beta = 1 + \frac{s_\gamma}{K} \quad \text{at } A_{\beta\gamma}, \tag{14a}$$

$$D_\beta \mathbf{n}_{\beta\gamma} \cdot \nabla s_\beta = D_\gamma \mathbf{n}_{\beta\gamma} \cdot \nabla s_\gamma \quad \text{at } A_{\beta\gamma}, \tag{14b}$$

$$\mathbf{n}_{\beta\sigma} \cdot \nabla s_\beta = 0 \quad \text{at } A_{\beta\sigma}, \tag{14c}$$

and the compatibility condition

$$\langle s_\beta \rangle = 0. \tag{15}$$

Similarly, variable s_γ of the γ-phase satisfies the following problem

$$D_\gamma \nabla^2 s_\gamma = -\varepsilon_\gamma^{-1} \alpha, \tag{16}$$

$$\mathbf{n}_{\gamma\sigma} \cdot \nabla s_\gamma = 0 \quad \text{at } A_{\gamma\sigma}, \tag{17}$$

$$\langle s_\gamma \rangle = 0, \tag{18}$$

where the mass-transfer coefficient, α, is given by

$$\alpha = \frac{D_\beta}{V} \int_{A_{\beta\gamma}} \mathbf{n}_{\beta\gamma} \cdot \nabla s_\beta \, \mathrm{d}A. \tag{19}$$

The above can be simplified by introducing the transformation $s_\beta = 1 + \alpha\psi_{\beta s}$ and $s_\gamma = \alpha\psi_{\gamma s}$, and in dimensionless form

$$s_\beta = 1 + \alpha^* \zeta_\beta, \tag{20a}$$

$$s_\gamma = \alpha^* \zeta_\gamma, \tag{20b}$$

where we defined the dimensionless mass-transfer coefficient $\alpha^* = a l_\beta^2 / D_\beta$, and l_β is a characteristic length of the β-phase. Then, in dimensionless notation, the boundary value problems read as follows: In the β-phase

$$Pe_\beta \mathbf{v} \cdot \nabla \zeta_\beta = \nabla^2 \zeta_\beta - \varepsilon_\beta^{-1}, \tag{21}$$

$$\mathbf{n}_{\beta\sigma} \cdot \nabla \zeta_\beta = 0 \quad \text{at } A_{\beta\sigma}, \tag{22}$$

where $Pe_\beta = \langle \mathbf{v} \rangle^\beta l_\beta / D_\beta$. In the γ-phase

$$0 = \delta \nabla^2 \zeta_\gamma + \varepsilon_\gamma^{-1}, \tag{23}$$

$$\mathbf{n}_{\gamma\sigma} \cdot \nabla \zeta_\gamma = 0 \quad \text{at } A_{\gamma\sigma}, \tag{24a}$$

$$\langle \zeta_\gamma \rangle = 0, \tag{24b}$$

where $\delta = D_\gamma / D_\beta$. The two problems are coupled at their interface through the condition

$$\zeta_\beta = \frac{1}{K} \zeta_\gamma \quad \text{at } A_{\beta\gamma}. \tag{25}$$

In this notation, the mass-transfer coefficient becomes

$$\alpha^* = -\frac{\varepsilon_\beta}{\langle \zeta_\beta \rangle}. \tag{26}$$

One final substitution will allow for additional insight. Define

$$\phi_\beta = \delta K \varepsilon_\gamma \zeta_\beta \tag{27a}$$

and

$$\phi_\gamma = \delta \varepsilon_\gamma \zeta_\gamma. \tag{27b}$$

Then, the two boundary value problems take the canonical form

$$Pe_\beta \mathbf{u} \cdot \nabla \phi_\beta = \nabla^2 \phi_\beta - \Lambda \quad \text{in the } \beta\text{-phase}, \tag{28}$$

$$\mathbf{n}_{\beta\sigma} \cdot \nabla \phi_\beta = 0 \quad \text{at } A_{\beta\sigma}, \tag{29}$$

where $\Lambda = \delta K \varepsilon_\gamma / \varepsilon_\beta$ and

$$0 = \nabla^2 \phi_\gamma + 1 \quad \text{in the } \gamma\text{-phase}, \tag{30}$$

$$\mathbf{n}_{\gamma\sigma} \cdot \nabla \phi_\gamma = 0 \quad \text{at } A_{\gamma\sigma}, \tag{31a}$$

$$\phi_\beta = \phi_\gamma \quad \text{at } A_{\beta\gamma}, \tag{31b}$$

$$\langle \phi_\gamma \rangle = 0. \tag{31c}$$

The mass-transfer coefficient is simply

$$\alpha^* = -\frac{\delta K \varepsilon_\beta \varepsilon_\gamma}{\langle \phi_\beta \rangle}. \tag{32}$$

Before proceeding with the analysis of the results, we note the following:

1. The overall problem is characterized by the geometry of the unit cell and by two dimensionless numbers, the Peclet number Pe_β and the dimensionless parameter Λ. The latter captures the ratio of diffusivities and the equilibrium partition constant in a single combination.
2. From Eqs. (28)–(31) we deduce $\langle \phi_\beta \rangle < 0$, indicating in (32) a positive mass-transfer coefficient, as expected.
3. The solution for ϕ_γ (Eqs. (30)–(31c)) is only geometry-dependent.

5. Asymptotic analysis

We will use the formulation given in Eqs. (28)–(32) to examine the following asymptotic limits:

a. *Limit* $Pe_\beta \ll 1$
In this limit, where the transport in the β-phase is diffusion-controlled, Eqs. (28)–(32) indicate that ϕ_β and ϕ_γ and, consequently, the mass transport coefficient α^* are independent of the velocity and the Peclet number Pe_β.

b. *Limit* $\Lambda = \delta K \varepsilon_\gamma / \varepsilon_\beta \ll 1$
In this limit, ϕ_β is geometry- and Peclet number-dependent. If we further assume geometric similarity (i.e., a constant ratio $\varepsilon_\beta / \varepsilon_\gamma$), we find the following scaling result:

$$\alpha^* \propto \delta K \varepsilon_\gamma \Rightarrow \alpha^* \propto \Lambda \varepsilon_\beta. \tag{33}$$

c. *Limit* $\Lambda = \delta K \varepsilon_\gamma / \varepsilon_\beta \gg 1$
This limit corresponds to the assumption of sufficiently fast diffusion in the γ-phase, frequently used in previous works. By substituting $\phi_\beta = \Lambda \eta_\beta$ in (28)–(29) the corresponding

boundary value problem in the β-phase now becomes

$$Pe_\beta \mathbf{u}\cdot\nabla\eta_\beta = \nabla^2\eta_\beta - 1, \tag{34}$$

$$\mathbf{n}_{\beta\sigma}\cdot\nabla\eta_\beta = 0 \quad \text{at } A_{\beta\sigma}, \tag{35a}$$

$$\eta_\beta = \frac{1}{\Lambda}\phi_\gamma \to 0 \quad \text{at } A_{\beta\gamma}. \tag{35b}$$

The solution for η_β is independent of Λ and depends only on Pe_β and the cell geometry. Thus, using the same approach as above, we find the scaling result

$$\alpha^* \propto \varepsilon_\beta. \tag{36}$$

This relation indicates the interesting result, that the mass transfer coefficient is independent of δ or K when Λ is large.

The above scaling relations will be checked against analytical solutions and numerical simulations to be reported below. Two different unit-cell geometries will be used: one involving two parallel phases of infinite extent, and another involving a unit cube with a disordered phase distribution.

6. Results

In the numerical simulations, the velocity field was computed numerically by solving the Stokes equations

$$\nabla p = \mu\nabla^2\mathbf{v}, \tag{37a}$$

$$\nabla\cdot\mathbf{v} = 0, \tag{37b}$$

$$\mathbf{v} = \mathbf{0} \quad \text{at } A_{\beta\sigma}, \tag{37c}$$

where $\mathbf{v}$, p, and μ are the velocity vector, the pressure field and the fluid viscosity, respectively. The procedure for solving the 3D Stokes flow problem involves discretization in terms of cubic elements and was as follows (Adler et al., 1990; Kikkinides and Burganos, 2000; Kainourgiakis et al., 2002; Coutelieris et al., 2003): At the pore level, a staggered marker-and-cell (MAC) mesh is used, with the pressure defined at the center of the cell and the velocity components defined along the corresponding face boundaries. The resulting linear system of equations is solved by a successive over-relaxation (SOR) method. An initial guess for p is determined through the solution of a Laplace equation. Next, the velocity vector $\mathbf{v}$ is calculated from the corresponding momentum balance and the continuity equation $\nabla\cdot\mathbf{v} = 0$. The pressure is corrected through an artificial compressibility equation of the form

$$\frac{\mathrm{d}p}{\mathrm{d}t} = \nabla\cdot\mathbf{v}. \tag{38}$$

Essentially, the method adds an artificial density time derivative related to the pressure by an artificial equation of state $p = \beta\rho$, where β is an artificial compressibility factor. In analogy with the compressible momentum equation, $c = \beta^{1/2}$ is an artificial speed of sound and thus for stability reasons during the iterative procedure, its magnitude should be such that the respective artificial Mach number, $M = \frac{R}{c}\max_D\left(\sum_i u_i^2\right)^{1/2}$ is low ($M \ll 1$), where R is the relevant Reynolds number. In the limiting case of $R \to 0$, which is the present case, any finite value of β should meet this criterion. Thus, we have chosen $\beta = 1$ although it is evident that the exact value cannot have any effect on the final (steady state) results since at steady state the artificial density time derivative is equal to zero.

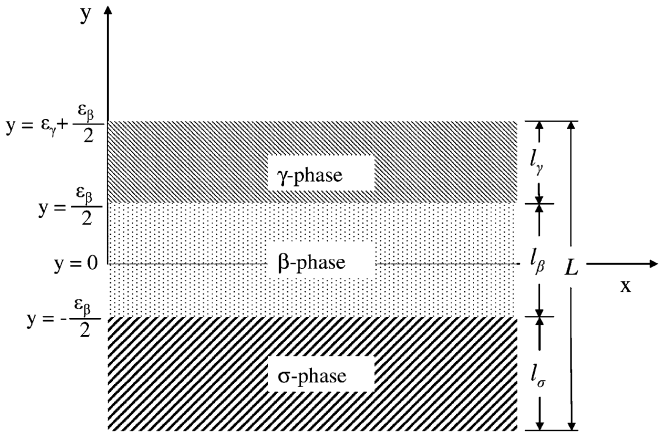

Fig. 2. A two-dimensional unit-cell for parallel phases.

The above steps are repeated until convergence is reached. This numerical scheme for the determination of the velocity field has been widely validated in terms of both the velocity field and the corresponding permeability (Adler et al., 1990; Kikkinides and Burganos, 2000; Kainourgiakis et al., 2002; Coutelieris et al., 2003).

For the numerical solution of the transport boundary value problems, a non-uniform finite differences scheme with upwinding was used for discretization, with the resulting linear systems of equations solved using again SOR.

6.1. Parallel phases

First, we solved the problem for the simplified geometry of parallel phases under the assumption of one-dimensional flow. In addition, it is considered that diffusion is significant only in the direction perpendicular to flow. These assumptions correspond to a *Pe*-independent Type II closure problem like that of Quintard and Whitaker (1994) for sufficiently fast diffusion. The unit cell is shown in Fig. 2 and has been used before to calculate properties of the Taylor-Aris dispersion problem for a passive tracer (Quintard and Whitaker, 1994). We solved the boundary value problem in this geometry analytically, yielding the following expression for the dimensionless mass-transfer coefficient

$$\alpha^* = \frac{\varepsilon_\beta\varepsilon_\gamma}{A_1 + A_2 + A_3}, \tag{39}$$

where we used as characteristic length the length L of the unit cell. (Note that in this notation we have $\alpha^* = \hat{\alpha}(l_\beta/L)^2$.) The coefficients are, respectively

$$A_1 = -\frac{1}{6\Lambda}\left[\left(\frac{\varepsilon_\beta}{2} + \varepsilon_\gamma\right)^3 - \frac{\varepsilon_\beta^3}{8}\right]\varepsilon_\beta^2, \tag{40a}$$

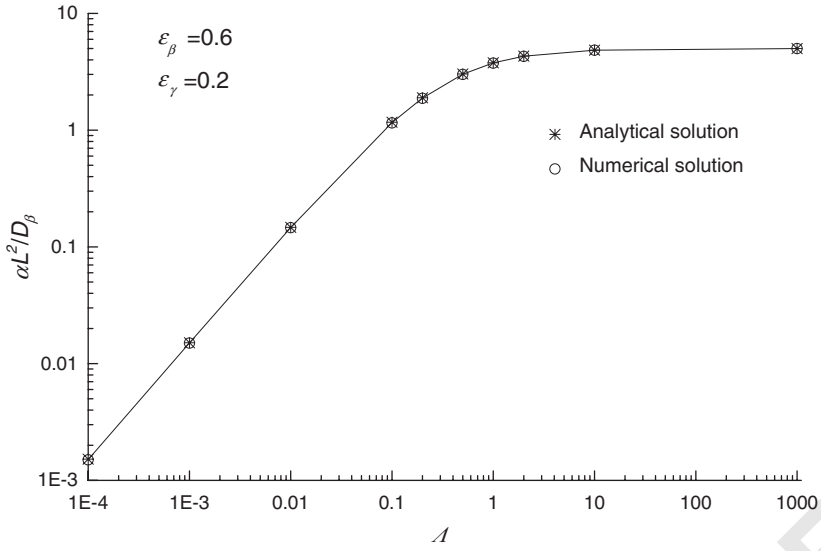

Fig. 3. Analytical and numerical results for the dimensionless mass-transfer coefficient for the case of parallel phases.

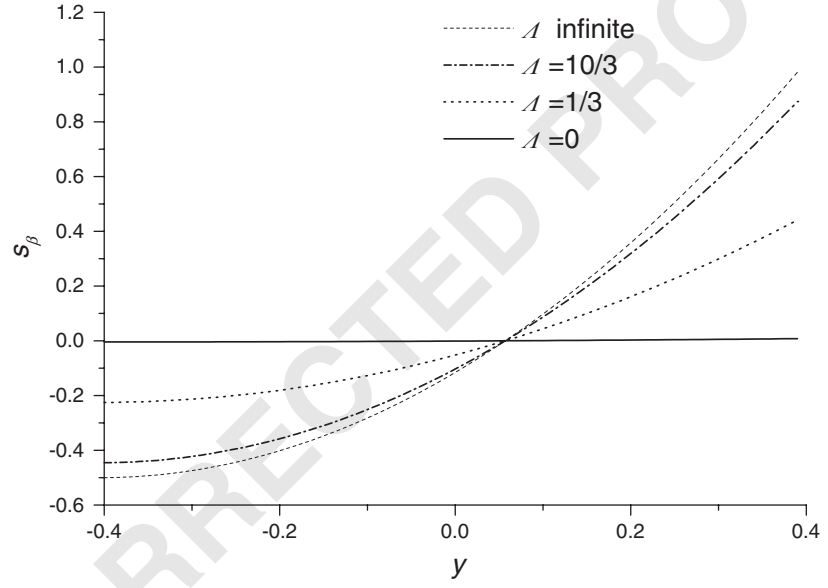

Fig. 4. Numerical results for s_β for the case of parallel phases.

$$A_2 = \frac{1}{2\Lambda}\left(1+\frac{\varepsilon_\beta}{2\varepsilon_\gamma}\right)\left[\left(\frac{\varepsilon_\beta}{2}+\varepsilon_\gamma\right)^2 - \frac{\varepsilon_\beta^2}{4}\right]\varepsilon_\gamma\varepsilon_\beta^2, \tag{40b}$$

$$A_3 = \frac{\varepsilon_\beta^4\varepsilon_\gamma}{3} - \left(\varepsilon_\gamma+\frac{\varepsilon_\beta}{4}\right)\frac{\varepsilon_\beta^3\varepsilon_\gamma}{2\Lambda}. \tag{40c}$$

In the limiting case of infinitely fast diffusion in the γ-phase ($\delta \to \infty \Rightarrow \Lambda \to \infty$), we find the asymptotic results $A_1 \to 0$, $A_2 \to 0$ and $A_3 \to \varepsilon_\beta^4\varepsilon_\gamma/3$, thus the dimensionless mass transport coefficient $\hat{\alpha} \to 3/\varepsilon_\beta$. This result coincides with the analytical mass transport coefficient for the case of parallel phases found in Quintard and Whitaker (1994) and shown to be independent of Peclet number. Fig. 3 shows the dimensionless mass transfer coefficient plotted as a function of the governing dimensionless parameter $\Lambda = \delta K\varepsilon_\gamma/\varepsilon_\beta$, calculated both by using the analytical approach and by numerical simulation. Analytical and numerical solutions are almost identical. For low values of Λ, the mass transfer coefficient increases with Λ (i.e., with increasing values of δ and/or K) in a linear fashion. At higher values, α reaches a constant value and becomes practically independent of Λ. This behavior is in agreement with the asymptotic analysis presented above (see Eq. (33) for low Λ and Eq. (36) for high Λ). The spatial distribution of the dimensionless scalar s_β is shown in Fig. 4. In the limiting case $\Lambda \to \infty \Rightarrow \delta \to \infty$ the calculated s_β values are identical to those found by Quintard and Whitaker

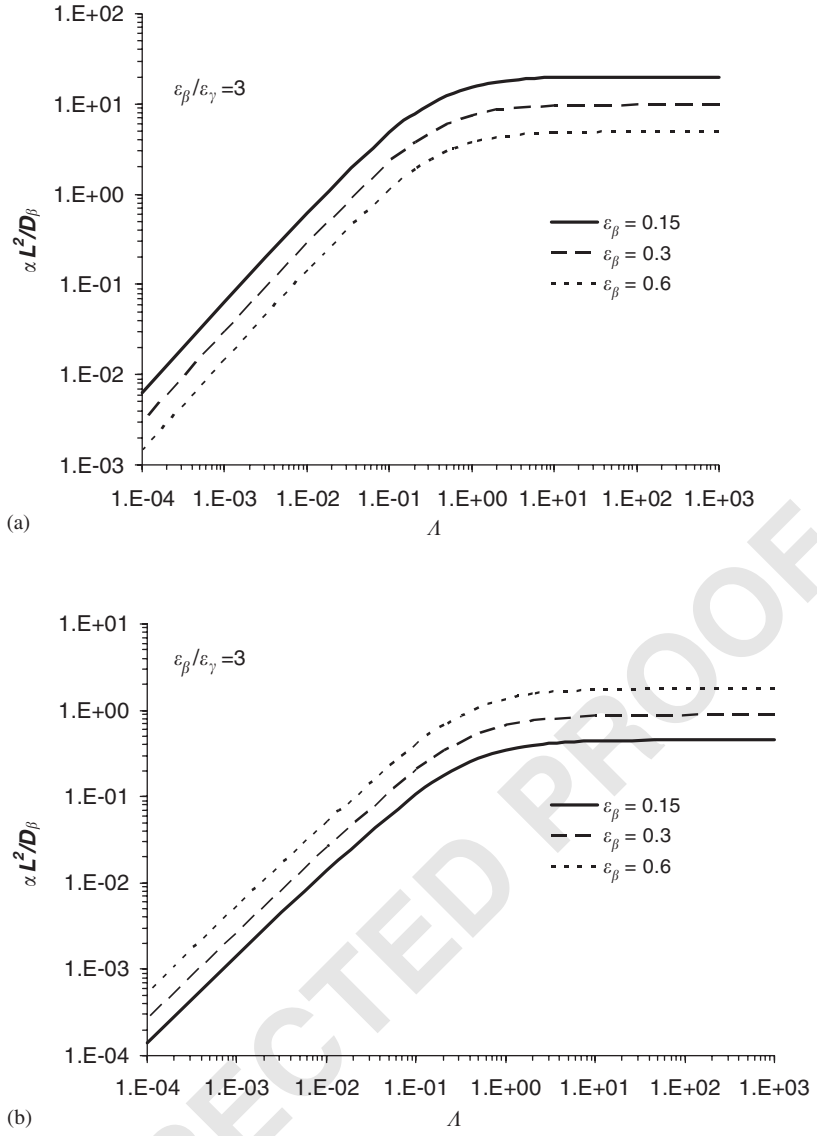

Fig. 5. The effect of Λ on the mass-transfer coefficient, defined either based on the characteristic length L (a) or on the characteristic length l_β (b) for various values of the volume fraction and for the case of parallel phases. Static conditions.

(1994) for fast diffusion in the γ-phase and for the same geometry.

Further probing of the validity of the asymptotic scaling results in this case is portrayed in Fig. 5, where the dimensionless mass-transfer coefficient is plotted against Λ for various values of the fraction ε_β, with the ratio $\varepsilon_\beta/\varepsilon_\gamma$ kept constant. In Fig. 5a, we used the length of the cell, $L = I_\sigma + I_\beta + I_\gamma$, as the characteristic length. The mass transfer coefficient $\hat{\alpha}$ is shown to decrease linearly with ε_β. Although in accordance with previous investigations (e.g. see Eq. (47e) in Quintard and Whitaker (1994)), this result seems at first inconsistent with the asymptotic analysis of Section 4, where a^* is predicted to increase linearly with ε_β. The explanation lies in the different characteristic lengths used to non-dimensionalize the mass-transfer coefficient. It is not difficult to show that for the parallel phases geometry we have $l_\beta/L = \varepsilon_\beta$, hence $a^* = \hat{a}\varepsilon^2\beta$. Fig. 5b shows the corresponding plot for a^* for various values of ε_β. An excellent agreement with the predictions of the asymptotic analysis is shown. In particular, $a^* \to 3\varepsilon_\beta$ when $\delta \to \infty \Leftrightarrow \Lambda \to \infty$, as expected.

6.2. Cubic unit cell

Next, we considered geometries that are more realistic than the limiting case of the parallel phases examined above. Fig. 6 shows a typical periodic 3-D unit cell, assumed to represent regularly packed granular porous media. The solid grains (σ-phase) are located at the eight edges of the cell. For the immobile γ-phase, two different cases are considered:

a. The immobile phase does not wet the solid, hence it is distributed in the pore space in the form of *blobs*.

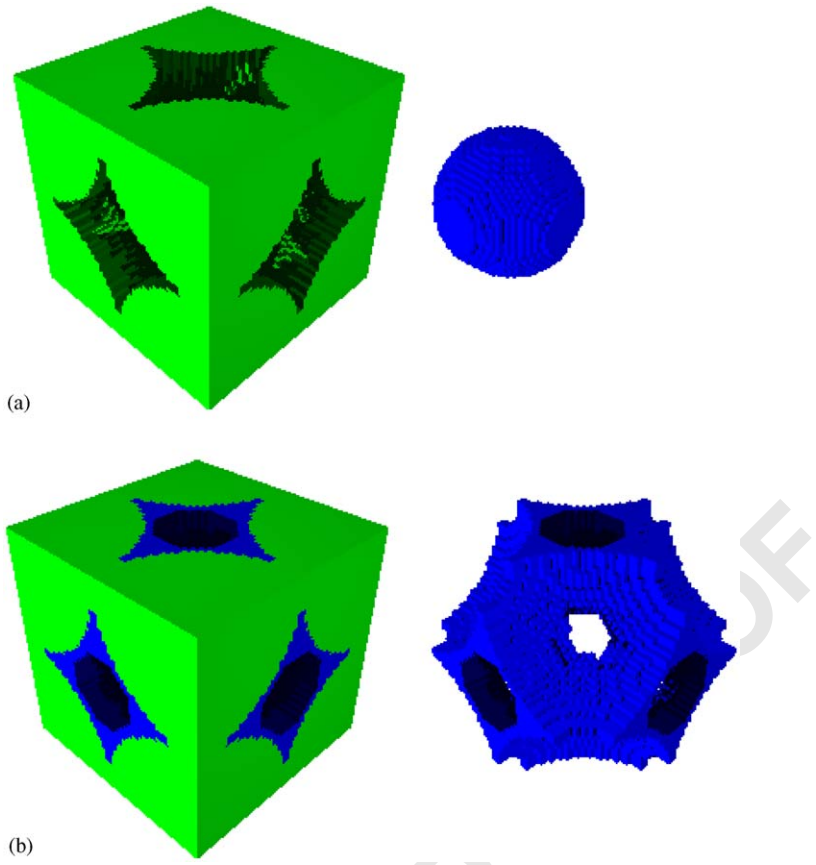

Fig. 6. A typical 3-D unit cell, with the immobile fluid phase configuration in the form of blobs (a) or films (b). Volume fractions $\varepsilon_\beta = 0.31$, $\varepsilon_\gamma = 0.12$. The immobile phase is also plotted separately for clarity.

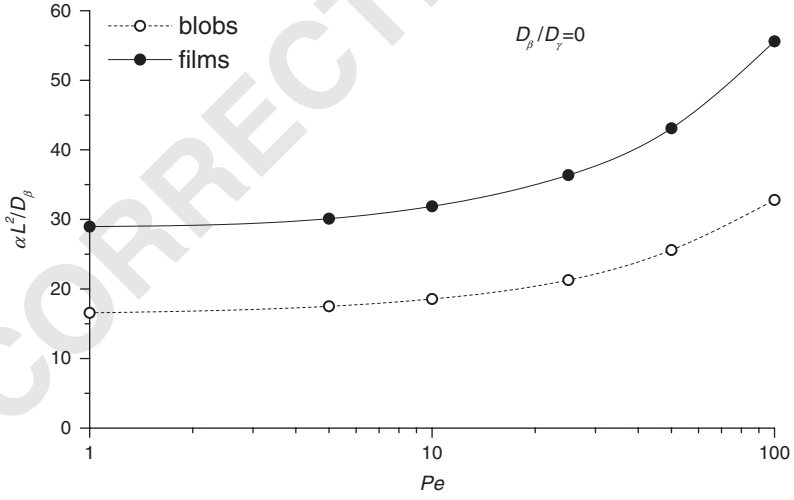

Fig. 7. The effect of the Peclet number on the mass-transfer coefficient for the limiting case of sufficiently fast diffusion in the γ-phase for the 3-D unit cell of Fig. 6.

b. The immobile phase wets the solid, hence it is distributed in the pore space in the form of *films*.

In either case, the "aqueous" phase (β-phase) flows under Stokes flow conditions. Initially, the case of infinitely fast diffusion in the γ-phase ($\delta = D_\gamma/D_\beta \to \infty$) is considered.

The effect of the pore-scale Peclet number on the dimensionless mass transfer coefficient is shown in Fig. 7 (for $\delta \to \infty$). As expected from the asymptotic analysis of Section 4, the mass-transfer coefficient is nearly constant at low Peclet numbers (of the order of less than unity), and starts increasing when the Peclet number increases. The wetting condition affects the

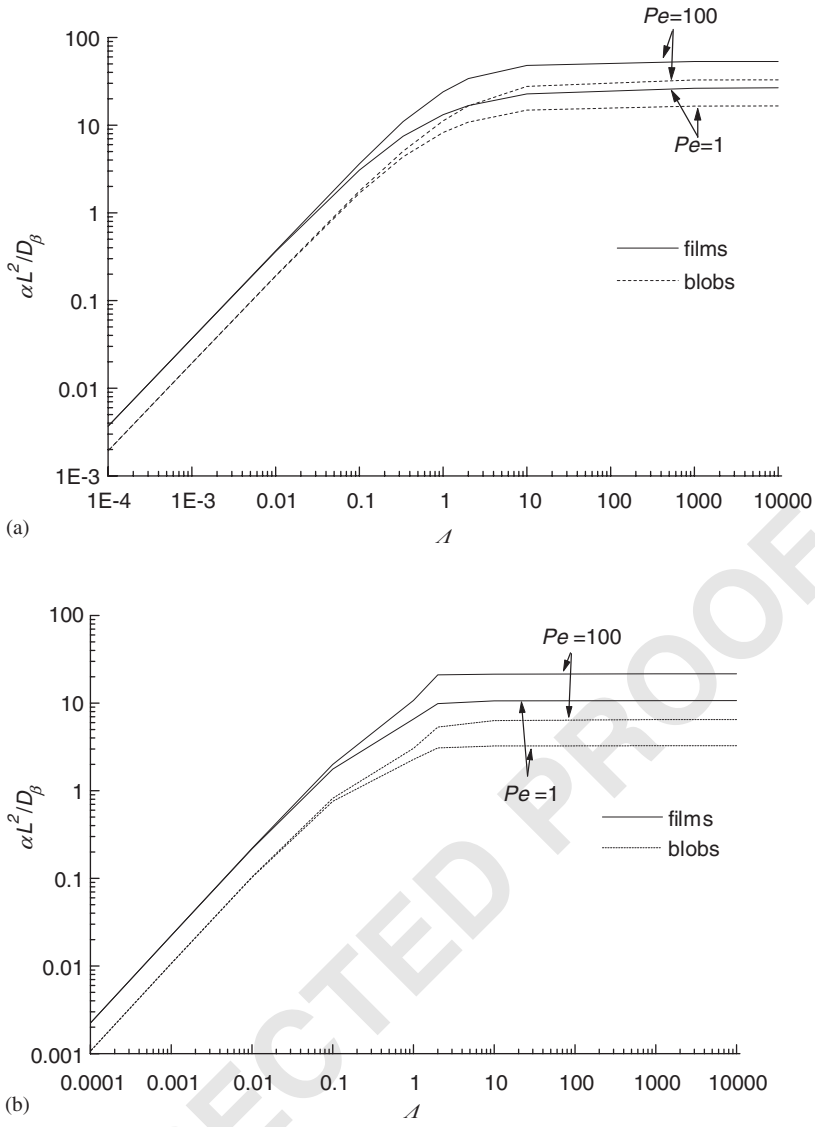

Fig. 8. The effect of Peclet number on the curve of the mass-transfer coefficient as a function of Λ. Two values are shown, one low ($Pe = 1$) and another high ($Pe = 100$). 3-D unit cells with volume fractions $\varepsilon_\beta = 0.31$ and $\varepsilon_\gamma = 0.12$ (a) and $\varepsilon_\beta = 0.39$ and $\varepsilon_\gamma = 0.04$ (b).

value of the mass transfer coefficient: the film (wetting) configuration of the immobile phase yields mass transfer coefficients always larger than those corresponding to blobs (non-wetting). This is a result of the higher surface area per unit volume available in the case of films in comparison to those of blobs for otherwise the same volumetric fractions. In addition, it should be noted that these results are in excellent agreement with the theoretical investigation of Ahmadi et al. (2001).

In Fig. 8, the effect of the dimensionless parameter Λ on the mass transfer coefficient is shown for two different values of the Peclet number. Again, in accordance with the asymptotic analysis of Section 4, the mass transport coefficient increases linearly with Λ at low Λ values, and reaches a constant value at high Λ. As before, the mass-transfer coefficient is higher in the case when the immobile phase is wetting (films) compared to the non-wetting case (blobs). The coefficient is independent of the Peclet number for low Λ values, also as predicted by the asymptotic analysis. When ε_β and ε_γ vary, the resulting trends are qualitatively similar, as observed from a direct comparison of Figs. 8a and b. We note that in these simulations, the dry porosity remains constant and equal to 0.43, ε_γ varied in the interval 0.12–0.4 and, consequently, ε_β varied in the interval 0.31–0.39. It is evident that as ε_γ decreases so does the mass-transfer coefficient.

Before proceeding further, it is important to stress once more the significance of parameter Λ. Indeed, one of the basic conclusions of this work is that through Λ we can reduce the parameters involved in the description of the process. For example, the diffusivity ratio δ has practically the same effect with the partitioning coefficient K, since $\Lambda = \delta K \varepsilon_\gamma / \varepsilon_\beta$. Similar conclusions can be drawn for the ratio of the phase porosities at least for well-defined geometries.

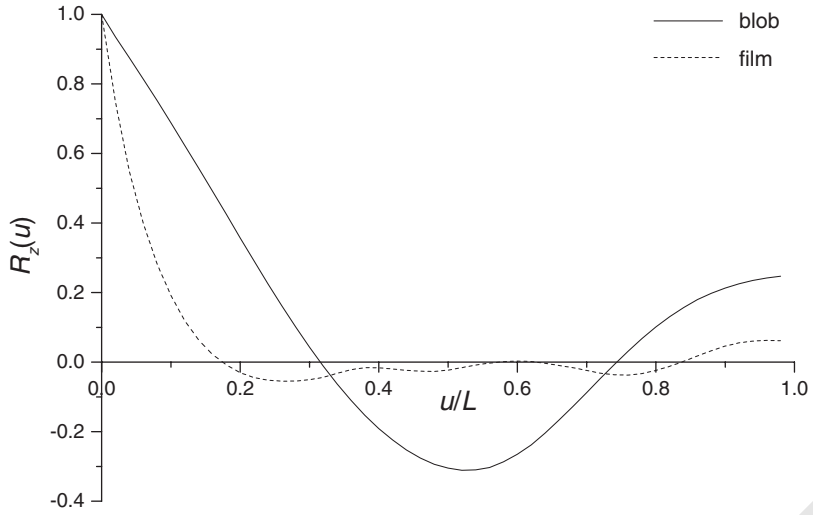

Fig. 9. Autocorrelation function of the wetting phase distribution $R_z(u)$.

7. Shape factors

The mass-transfer coefficient has been explicitly described in the literature as a function of the geometry and the physicochemical characteristics of the immobile phase, using expressions of the form

$$a = \beta \frac{\varepsilon_\beta D_\beta}{b^2}, \tag{41}$$

where b is a characteristic length scale and the unknown shape factor β is geometry-dependent (Van Genuchten and Wierenga, 1976; Goltz and Roberts, 1988; Parker and Valocchi, 1986; Cherblanc et al., 2003). The numerical results of the present study can be used to calculate the shape factor for the various geometries investigated. In the case of parallel phases, we find numerically that β has the value 3.04, which is in excellent agreement with the theoretical value $\beta = 3$ corresponding to 1-D diffusion in a slab (Cherblanc et al., 2003).

For the case of a 3-D unit cell, where the immobile phase is in the form of a spherical blob (see Fig. 6), the calculated value under static conditions is $\beta = 14.97$, which is again in excellent agreement with the theoretical value $\beta = 15$, obtained for 3-D diffusion in a sphere representing 3-D heterogeneity (Parker and Valocchi, 1986). The case of a wetting immobile phase (films) is not as straightforward, however, due to the complex geometry of the films (Fig. 6). To extract the characteristic length of the immobile phase in this case, we used the following approach: First, we calculated the two-point autocorrelation function of the immobile phase alone and defined the characteristic length as the shortest distance at which the two-point autocorrelation function becomes equal to zero (Fig. 9). For a blob-like distribution, this length is equal to the radius of the spherical blob (e.g. see (Torquato, 2002)), as can be seen from the same Fig. 9. After determining the respective length for the case of films, we find that in the static case $\beta = 9.1$, a value that is closer to the one for radial diffusion in an infinite cylinder ($\beta = 8$) and which represents 2-D heterogeneity. This can be understood from the fact that an immobile phase in the form of films resembles in some sense the shape of a 2-D wafer, slightly distorted due to the disorder in the unit cell. As a result, a certain degree of 3-D heterogeneity is induced, thus altering the shape factor to somewhat larger values than the ones corresponding to the pure 2D case.

8. Conclusions

In this paper we derived the effective mass-transfer coefficient between two fluid phases in a porous medium, one of which is flowing and the other is immobile. A passive tracer is advected by the flowing phase, becomes partitioned at the fluid–fluid interface and diffuses in the immobile phase. We used traditional volume-averaging methods to obtain a unit-cell boundary-value problem for the calculation of the effective mass-transfer coefficient. The problem was shown to be controlled by the Peclet number of the flowing phase, the dimensionless parameter $\Lambda = \delta K \varepsilon_\gamma / \varepsilon_\beta$, that captures diffusion and partition in the two phases and the geometrical properties of the porous medium.

We derived asymptotic results for the scaling of the mass-transfer coefficient under various limiting conditions. Then, we used numerical methods that solve for the flow velocity field under Stokes flow conditions, and for the transport problem. The numerical results verify the asymptotic scaling expressions and provide estimates of the coefficient for a number of special cases. In particular, we found that when the immobile phase is wetting the solid (in the form of films), the mass-transfer coefficient is larger than in the non-wetting case (where the phase is distributed in the form of blobs). Shape factors for practical applications were also obtained.

The results generalize the effective mass-transfer coefficient when the assumption of infinitely fast diffusion in the immobile phase breaks down. The value of the coefficient is smaller than in the case of infinitely fast diffusion, and in fact vanishes as the product of the partition coefficient and the diffusivity

ratio vanishes. The effect of the Peclet number is significant at high value of parameter Λ (namely at fast diffusion) but less important at lower values.

Notation

A_1, A_2, A_3	dummy variables used in Eq. (40)
$A_{\beta\gamma}, A_{\beta\sigma}, A_{\gamma\sigma}$	area of the β–γ, β–σ and γ–σ interfaces, respectively
b	characteristic length scale
$\mathbf{b}_\beta, \mathbf{b}_\gamma$	vectors satisfy closure problems in the β- and γ-phase, respectively
C_β, C_γ	concentrations of diffusing species in the β- and γ-phase, respectively
C'_β, C'_γ	fluctuations used for the decomposition of the concentrations in the β- and γ-phase, respectively
D_β, D_γ	molecular diffusivities of diffusing species in the β- and γ-phase, respectively
D^*_β, D^*_γ	dispersivities in the β- and γ-phase, respectively
K	partitioning coefficient
$l_\beta, l_\gamma, l_\sigma$	characteristic length of β-, γ-and σ-phases, respectively
L	total length of the unit cell
$\mathbf{n}_{\beta\gamma}, \mathbf{n}_{\beta\sigma}, \mathbf{n}_{\gamma\sigma}$	unit normal vectors directed from β-phase to γ-phase, from β-phase to σ-phase and from γ-phase to σ-phase, respectively
p	pressure field of flowing β-phase
Pe	Peclet number $[=\langle\mathbf{v}\rangle^\beta L/D_\beta]$
Pe_β	Peclet number defined in the β-phase $[=\langle\mathbf{v}\rangle^\beta l_\beta/D_\beta]$
s_β, s_γ	dimensionless scalars for the closure problems in the β- and γ-phase, respectively
t	time
$\mathbf{v}_\beta$	velocity-like coefficient used in the velocity averaged transport equations in the β-phase
$\mathbf{v}$	velocity in the β-phase
$\mathbf{v}'_\beta$	fluctuation used for the decompositions of the velocity in the β-phase
V	total volume
V_β, V_γ	volume of β- and γ-phase, respectively
y_i	$(i=\beta, \gamma, \sigma)$ dummy quantity associated with phase i

Greek letters

α	mass transport coefficient
α^*	dimensionless mass transport coefficient $[=al^2_\beta/D_\beta]$
$\hat{\alpha}$	dimensionless mass transport coefficient $[=aL^2/D_\beta]$
β	geometry-dependent shape factor used in Eq. (41)
δ	diffusivity ratio $[=D_\gamma/D_\beta]$
$\varepsilon_\beta, \varepsilon_\gamma$	volume fraction of the β- and γ-phase, respectively
$\zeta_\beta, \zeta_\gamma$	scalar variables used for the asymptotic analysis
η_β	scalar variable used for the asymptotic analysis when $\Lambda \gg 1$
Λ	dimensionless parameter $[=\delta K\varepsilon_\gamma/\varepsilon_\beta]$
μ	viscosity of flowing β-phase
ξ	parameter used for the decomposition of s_β and s_γ
ϕ_β, ϕ_γ	scalar variables used for the decomposition of ζ_β and ζ_γ
$\psi_{\beta s}, \psi_{\gamma s}$	scalar variables used for the decomposition of $\mathbf{b}_\beta$, s_β and $\mathbf{b}_\gamma$, s_γ, respectively

Subscripts/superscripts

β	indicator of the flowing aqueousphase
γ	indicator of the trapped non-aqueous liquid phase
σ	indicator for the solid phase

Other symbols

$\langle Q\rangle$	superficial volume average of any quantity Q
$\langle Q\rangle^i$	$(i=\beta, \gamma, \sigma)$ interstitial volume average of any quantity Q in the phase i

Acknowledgment

Partial funding by the European Commission DG Research contract ENK6-CT-2002-00602 ENVITRACER is gratefully acknowledged by the authors.

References

Adler, P.M., Jacquin, C.J., Quiblier, J.A., 1990. Flow in simulated porous media. International Journal of Multiphase Flow 16, 691–712.

Ahmadi, A., Quintard, M., Whitaker, S., 1998. Transport in chemically and mechanically heterogeneous porous media V: two-equation model for solute transport with adsorption. Advance in Water Resource 22, 59–86.

Ahmadi, A., Aigueperse, A., Quintard, M., 2001. Calculation of the effective properties describing active dispersion in porous media: from simple to complex porous media. Advances in Water Resource 24, 423–438.

Bekri, S., Adler, P.M., 2002. Dispersion in multiphase flow through porous media. International Journal of Multiphase Flow 28, 665–697.

Bekri, S., Thovert, J.-F., Adler, P.M., 1997. Dissolution and deposition in fractures. Engineering Geology 48, 283–308.

Carbonell, R.G., Whitaker, S., 1984. Heat and mass transfer in porous media. In: Bear, J., Carpacioglu, M.Y. (Eds.), Fundamentals of Transport Phenomena in Porous Media. Martinus Nijhof Publ., Dordrecht, The Netherlands, pp. 121–198.

Cherblanc, F., Ahmadi, A., Quintard, M., 2003. Two-medium description of dispersion in heterogeneous porous media: calculation of macroscopic properties. Water Resource Research 39, 1154–1174.

Coutelieris, F.A., Kainourgiakis, M.E., Stubos, A.K., 2003. Low Peclet mass transport in assemblages of spherical particles for two different adsorption mechanisms. Journal of Colloid and Interface Science 264, 20–29.

Dagan, G., Lessoff, S., 2001. Solute transport in heterogeneous formations of bimodal conductivity distribution: 1. Theory. Water Resource Research 37, 465–472.

De Smedt, F., Wierenga, P.J., 1979. A generalized solution for solute flow in soils with mobile and immobile water. Water Resource Research 15, 1137–1141.

Fried, J.J., Muntzer, P., Zilliox, L., 1979. Groundwater pollution by transfer of oil-hydrocarbons. Ground Water 17, 586–594.

Geller, J.T., Hunt, J.R., 1993. Mass transfer from non-aqueous phase organic liquids in water-saturated porous media. Water Resource Research 29, 833–845.

Goltz, M.N., Roberts, P.V., 1988. Simulations of physical non-equilibrium solute transport models: application to a large-scale field experiment. Journal of Contaminant Hydrology 3, 37–63.

Gvirtzam, H., Paldor, N., Magaritz, M., Bachmat, Y., 1988. Mass exchange between mobile freshwater and immobile saline water in the unsaturated zone. Water Resource Research 24, 1638–1644.

Gwo, J.-P., O'Brien, R., Jardine, P.M., 1998. Mass transfer in structured porous media: embedding mesoscale structure and microscale hydrodynamics in a two-region model. Journal of Hydrology 208, 204–222.

Hunt, J.R., Sitar, N., Udell, K.S., 1988. Non-aqueous phase liquid transport and cleanup I: analysis of mechanisms. Water Resource Research 24, 1247–1258.

Kainourgiakis, M.E., Kikkinides, E.S., Stubos, A.K., 2002. Diffusion and flow in porous domains constructed using process-based and stochastic techniques. Journal of Porous Materials 9, 141–154.

Kechagia, P.E., Tsimpanogiannis, I.N., Yortsos, Y.C., Lichtner, P.C., 2002. On the upscaling of reaction-transport processes in porous media with fast or finite kinetics. Chemical Engineering & Science 57, 2565–2577.

Kikkinides, E.S., Burganos, V.N., 2000. Permeation properties of three-dimensional self-affine reconstructions of porous materials. Physical Review E 62, 6906–6915.

Lam, A.C., Schechter, R.S., Wade, W.H., 1983. Mobilization of residual oil under equilibrium and non-equilibrium conditions. Society of Petroleum Engineers Journal 23, 781–790.

Lessoff, S., Dagan, G., 2001. Solute transport in heterogeneous formations of bimodal conductivity distribution: 2. applications. Water Resource Research 37, 473–480.

Parker, J.C., Valocchi, A.J., 1986. Constraints on the validity of equilibrium and first-order kinetic transport models in structured soils. Water Resource Research 22, 399–407.

Plumb, O.A., Whitaker, S., 1990. Diffusion, adsorption and dispersion in heterogeneous porous media: the method of large scale averaging. In: Cushman, J.H. (Ed.), Dynamics of Fluids in Hierarchical Porous Media. Academic Press, NY, USA. (Chapter VI).

Quintard, M., Whitaker, S., 1993a. One and two equation models for transient diffusion processes in two-phases systems. Advances in Heat Transfer 23, 369–464.

Quintard, M., Whitaker, S., 1993b. Transport in ordered and disordered porous media: volume averaged equations, closure problems and comparison with experiments. Chemical Engineering & Science 48, 2537–2564.

Quintard, M., Whitaker, S., 1994. Convection dispersion and interfacial transport of contaminants: homogeneous porous media. Advances in Water Resource 17, 221–239.

Torquato, S., 2002. Random Heterogeneous Materials: microstructure and Macroscopic Properties. Springer, New York.

Van Genuchten, M.T., Wierenga, P.J., 1976. Mass transfer studies in sorbing porous media i. Analytical solutions. Soil Science Society of American Journal 40, 180–473.

Vogel, T., Gerke, H., Zhang, R., Genuchten, M.V., 2000. Modeling flow and transport in a two-dimensional dual-permeability system with spatially variable hydraulic properties. Journal of Hydrology 238, 78–89.

Whitaker, S., 1967. Diffusion and dispersion in porous media. A.I.Ch.E. Journal 13, 420–427.

Whitaker, S., 1977. Simultaneous heat, mass and momentum transfer in porous media: a theory of drying. In: Advances in Heat Transfer, vol. 13. Academic Press, NY, USA, pp. 119–203.

Zanotti, F., Carbonell, R.G., 1984a. Development of transport equations for multiphase systems I: general development for two-phase systems. Chemical Engineering & Science 39, 263–278.

Zanotti, F., Carbonell, R.G., 1984b. Development of transport equations for multiphase systems II: application to one-dimensional axi-symmetric flows of two-phases. Chemical Engineering & Science 39, 279–297.